

ORIGINAL ARTICLE

Analysis of the phosphoproteome in human dental follicle cells during osteogenic differentiation

Christian Morszeck¹  | Oliver Pieleś¹  | Hans-Christian Beck² 

¹Department of Oral and Maxillofacial Surgery, University Hospital Regensburg, Regensburg, Germany

²Department of Clinical Biochemistry and Pharmacology, Centre for Clinical Proteomics, Odense University Hospital, Odense, Denmark

Correspondence

Christian Morszeck, University Hospital Regensburg, Department of Oral and Maxillofacial Surgery, Franz-Josef-Strauss-Allee 11, 93053 Regensburg, Germany.
Email: christian.morszeck@ukr.de

Funding information

Deutsche Forschungsgemeinschaft, Grant/Award Number: 319390412

Abstract

Dental follicle cells (DFCs) are osteogenic progenitor cells and are well suited for molecular studies of differentiation of alveolar osteoblasts. A recent study examined the metabolism in DFCs during osteogenic differentiation and showed that energy metabolism is increased after 14 days of differentiation (mid phase). However, previous studies have examined proteomes at early (2 h, 24 h) or very late (28 days) stages of differentiation, but not during the phase of increased metabolic activity. In this study, we examined the phosphoproteome at the mid phase (14 days) of osteogenic differentiation. Analysis of DFC phosphoproteomes showed that during this phase of osteogenic differentiation, proteins that are part of signal transduction are significantly regulated. Proteins involved in the regulation of the cytoskeleton and apoptosis were also increased in expression. As osteogenic differentiation induced oxidative stress and apoptosis in DFCs, the oxidative stress defense protein, catalase, was also upregulated during osteogenic differentiation, which supports the biomineralization of DFCs. In summary, this study revealed that during the middle phase (14 days) of osteogenic differentiation, processes in DFCs related to the control of cell organization, apoptosis, and oxidative stress are regulated.

KEYWORDS

dental stem cells, development, mineralization

INTRODUCTION

The dental follicle is a tooth germ tissue that contains undifferentiated progenitor cells destined for the periodontium [1, 2]. From the dental follicle, mesenchymal stem cells (dental follicle cells [DFCs]) can be isolated as plastic adherent colony-forming cells that have, for example, good osteogenic differentiation potential [3–5]. Early investigations of DFCs showed that osteogenic differentiation can be induced after activation of the bone morphogenetic protein (BMP) pathway

via BMP-2 [5, 6]. In addition, the transcription factor, homeobox protein DLX3 (DLX3), from the distal-less homeobox protein family, is activated downstream of the BMP pathway [7–9]. This BMP/DLX3 pathway induces osteogenic differentiation markers, such as alkaline phosphatase (ALP) activity [9, 10]. However, the molecular mechanisms downstream of the induction of the osteogenic differentiation by BMP-2 are complex [11]. For example, a previous study from our group investigated the mechanisms that took place 2 and 24 h after induction of osteogenic differentiation by BMP-2 [12].

This is an open access article under the terms of the [Creative Commons Attribution-NonCommercial License](https://creativecommons.org/licenses/by-nc/4.0/), which permits use, distribution and reproduction in any medium, provided the original work is properly cited and is not used for commercial purposes.

© 2023 The Authors. *European Journal of Oral Sciences* published by John Wiley & Sons Ltd on behalf of Scandinavian Division of the International Association for Dental Research.

We have shown that off-state hedgehog phosphoproteins, which are associated with an inactivated state of hedgehog signaling, are differentially expressed. Bone morphogenetic protein 2 induced the expression of hedgehog-signaling pathway repressors, such as Patched 1 (PTCH1), suppressor of fused homolog (SUFUH), and parathyroid hormone-related protein (PTHrP). The repressor, PTHrP, plays two different roles in osteogenic differentiation: while secreted PTHrP regulates ALP activity and DLX3 expression in DFCs [13], high endogenous expression of PTHrP correlates strongly with induced enhanced osteogenic differentiation potential [14]. In a recent study, we showed that classical protein kinases (protein kinase C [PKC]), such as protein kinase C alpha type (PKC-A), inhibit osteogenic differentiation of DFCs [15]. The expression of PKCs is down-regulated after 7 days and later by osteogenic differentiation [15]. Protein kinase Cs also affect expression of protein kinase B (the collective name for a set of three serine/threonine protein kinases known as AKT1), which is down-regulated in the later stages (day 7 and subsequently) of BMP-2-induced differentiation. Regulation of this PKC/AKT axis supports the biomineralization of DFCs by inhibiting the nuclear factor kappa-light-chain-enhancer of activated B cell (NF- κ B) signaling [15]. Interestingly, it is also known that during osteogenic differentiation, when the signaling pathways mentioned here are regulated in the DFCs, metabolic processes in the cell also change. Recent studies found that lipid synthesis (for example, of cholesterol) and other metabolic processes are also involved in the later stages of osteogenic differentiation (14 days after induction) [16, 17]. Moreover, inhibition of fatty acid synthesis decreased the osteogenic differentiation potential of DFCs [17]. The present study also shows that oxidative stress is induced during osteogenic differentiation. It is therefore evident that the control of oxidative stress or reactive oxygen species (ROS), as second messengers, is essential for differentiation.

Other molecular processes must be involved in the induction/regulation of mineralization and metabolic processes, both of which are induced 14 days after osteogenic differentiation [17]. In the present study, we therefore examined phosphorylated proteins in the proteome (phosphoproteome) of DFCs 14 days after induction of osteogenic differentiation and identified regulated proteins belonging to signaling pathways associated with the Rho-GTPase cycle and apoptosis.

MATERIAL AND METHODS

Cell culture

Human DFCs were obtained commercially (AllCells). The standard culture medium was Dulbecco's modified Eagle's

medium (DMEM; Sigma–Aldrich) supplemented with 10% fetal bovine serum (FBS; Sigma–Aldrich) and 100 μ g mL⁻¹ of penicillin/streptomycin. Dental follicle cells at passage 6 were used for experiments.

Osteogenic differentiation

The DFCs were cultured in DMEM until subconfluent (>80%), then osteogenic differentiation was stimulated with osteogenic differentiation medium. Two differentiation media, designated BMP-2 and ODM, were used. The BMP-2 medium is a DMEM-based cell culture medium containing 2% FBS (Sigma–Aldrich), 100 μ mol L⁻¹ of ascorbic acid-2-phosphate, 10 mmol L⁻¹ of KH₂PO₄, 20 mmol L⁻¹ of HEPES, 50 ng mL⁻¹ of BMP-2, and 100 μ g mL⁻¹ of penicillin/streptomycin (Sigma Aldrich). Osteogenic differentiation medium (ODM) does not contain BMP-2, but 10 nM dexamethasone. 3-amino-1,2,4-triazole (3-AT; Sigma Aldrich) was used to inhibit catalase and MK2206 (Sigma Aldrich) was used to inhibit AKT. The differentiation of DFCs was assessed by evaluating the degree of mineralization of the extracellular matrix using alizarin red staining. Cells were fixed with 4% formalin and stained using Alizarin Red Solution (Merck). The stains were quantified by dissolving alizarin red crystals in cetylpyridinium chloride and measuring the optical density at 595 nm.

Isolation of total proteins

For analysis of the phosphoproteome, DFCs were cultivated in BMP-2 or ODM. As a control, DFCs were cultured in standard medium DMEM. Total proteins were isolated 14 days after induction of osteogenic differentiation.

Protein extraction was performed as follows. DFCs were harvested by trypsin-treatment. The cells were lysed in buffer (20 mM Tris, 48 mM NaF, 150 mM NaCl, 2 mM sodium orthovanadate, 1% Nonidet P-40 [NP-40], and 10% glycerol) containing protease (Roche) and phosphatase (Sigma) inhibitor cocktails (freshly made according to the manufacturers' instructions), and incubated on ice for 30 min. Soluble proteins were isolated after centrifugation (5 min; 14,000 g).

Oxidative stress

Oxidative stress was estimated using the GSH/GSSG-Glo Assay Kit (Promega) according to the manufacturer's instructions. This assay measures the amounts of oxidized and reduced glutathione in DFCs. For each experimental group, three biological replicates were used. The relative amount was

calibrated to the amount of oxidized and reduced glutathione in untreated DFCs.

A flow cytometry-based assay was used to detect reactive oxidative species (ROS). The DFCs were washed with PBS, trypsinized, centrifuged, and resuspended in the same medium used previously in the experiment but this time with the addition of 20 μM 2',7'-dichlorofluorescein diacetate (H2DCFDA; Sigma-Aldrich). Subsequently, the cells were incubated for 30 min at 37°C and 5% CO₂ in a humidified atmosphere and then analyzed using a FACSCanto II (Becton Dickinson). Fluorescence detected in the fluorescein isothiocyanate (FITC) channel was used as a measure of oxidative stress. Cells that were simultaneously processed without H2DCFDA served as the negative control. FLOWING SOFTWARE 2 (Version 2.5.1, Perrtu Terho, Turku Bioscience) was used for flow data analysis.

Quantitative Reverse Transcription PCR

Total RNA was isolated from cells using the RNeasy isolation kit (Qiagen). cDNA synthesis was performed using total RNA and the iScript Advanced cDNA Synthesis Kit for RT-qPCR (Bio-Rad), according to the manufacturer's protocol. The PCR cycling was performed using SsoAdvanced Universal SYBR Green Supermix (Bio-Rad) in the StepOne Real-Time PCR machine (Life Technology). Primers for the catalase gene (*CAT*) were purchased from Bio-Rad. For relative gene expression in a single sample, expression of *CAT* was normalized to expression of the glyceraldehyde-3-phosphate dehydrogenase gene (*GAPDH*) (housekeeping gene) and calibrated to the relative gene expression in a control group using the $\Delta\Delta\text{Ct}$ method [18].

Apoptosis assay

Apoptotic and dead cells were evaluated using the Cell Event Caspase-3/7 Green Flow Cytometry Assay (Life Technologies). Dental follicle cells were harvested using trypsin-EDTA treatment, washed with PBS, and stained with Caspase-3/7 Green Detection Reagent (25 min, 37°C). Then, 1 mM SYTOX AADvanced staining solution was added to the dead cell sample. Cell fluorescence was analyzed at 488 nm excitation and applied to standard fluorescence compensation. Fluorescence emission was measured using 530/30 BP (for Caspase-3/7 Green Detection Reagent) and 690/50 BP (for SYTOX AADvanced dead cell dye) filters. Apoptotic cells stained positive with Caspase-3/7 Green Detection Reagent and dead cells stained positive with SYTOX AADvanced Dead Cell Stain. By contrast, vital cells stained negative following application of these stains.

Phosphoproteomic analysis

Precipitated protein extracts were reduced, blocked with iodoacetamide, trypsinized, and labeled with the 16-plex tandem mass tag (TMT) reagent, according to the manufacturer's protocol (Thermo Scientific). Controls and samples were tagged with mass tags 127N through 134N and compared with a pool of all samples (mass tag 126). The resulting peptide mixtures (ca. 400 μg) were subjected to phosphopeptide enrichment using titanium dioxide (TiO₂), virtually as previously described (PMID: 28,116,542). The purified phosphopeptide mixtures were fractionated into seven fractions using high pH fractionation, also as previously described (PMID: 34,941,812), and analyzed using nanoscale liquid chromatography coupled to tandem mass spectrometry (nano-LC-MS/MS), as described below.

Nano-LC-MS/MS analysis was performed on a Orbitrap Exploris 480 mass spectrometer (Thermo Fisher Scientific) equipped with a nanoflow high-performance liquid chromatography (nano-HPLC) interface (Dionex UltiMate 3000 nano HPLC). Samples (5 μL) were loaded for 7 min with a flow rate of 4 $\mu\text{L min}^{-1}$ onto a custom fused capillary guard column (2 cm length, 360 μm OD, 75 μm ID, packed with ReproSil Pur C18 5 μm resin [Dr Maish]). Captured peptides were separated on a custom-designed fused capillary column (20 cm length, 360 μm OD, 75 μm ID, packed with ReproSil Pur C18 1.9 μm resin) using a linear gradient from 90% to 86% buffer A (0.1% formic acid) to 27% to 32% buffer B (80% acetonitrile in 0.1% formic acid) over 40 min with a flow rate of 250 nL min^{-1} . Mass spectra were acquired in positive ion mode, using automatic data-dependent switching between an Orbitrap MS scan in the 350–1400 m/z mass range followed by high-energy collision dissociation (HCD) fragmentation of selected peptide followed by detection of fragmented peptide ions using an Orbitrap. The normalized AGC target for MS1 was 200% at 60-kDa resolution, and the normalized AGC target for MS2 was 200% at 45-kDa resolution. The isolation window was 0.7 Da. Fragmentation in the HCD cell was performed at normalized collision energies of 35 eV. The ion selection threshold was 20,000 counts, and selected sequenced ions were dynamically excluded for 60 s.

All Exploris raw data files were processed and quantified using PROTEOME DISCOVERER VERSION 2.4.1.15 (Thermo Scientific). The SEQUEST SEARCH ENGINE built into PROTEOME DISCOVERER was used to search the data using the following criteria—Protein Database: Uniprot (downloaded September 30, 2019, 42,369 entries) and restricted to humans. Fixed search parameters included trypsin, allowing a missed cleavage, carbamidomethylation at cysteines, and TMTpro (Thermo) labeling at lysine and N-terminal amines, while serine, threonine, and tyrosine phosphorylation, methionine

oxidation, and deamidation were set as dynamic. The mass tolerance of the precursor was adjusted to 8 ppm and the mass tolerance of the fragment was adjusted to 0.05 Da. A false discovery rate (FDR) was calculated using a decoy database search, and only peptide identifications with high confidence (misrecognition rate < 1%) were included.

The regulated phosphoprotein peptides identified from different groups were compared and selected according to statistical significance (Student's *t*-test $p < 0.05$; ratio > 2 (up-regulated) or ratio < 0.5 (down-regulated)) and were compared with analysis databases Reactome (reactome.org) and DAVID Bioinformatics Resources (david.ncifcrf.gov) [19, 20].

Statistical analyses

The statistical analyses for phosphoproteomics data are described above. For further statistical analysis, the results were analyzed using SPSS 23 STATISTICAL SOFTWARE (SPSS). Statistical analyses were performed using the Student's *t*-test. A value of $p < 0.05$ was considered to indicate statistical significance.

RESULTS

Proteomics results

Phosphoproteomes were analyzed 14 days following induction of osteogenic differentiation with BMP-2 or dexamethasone (ODM). They were compared with the phosphoproteome of DFCs cultured in standard medium for 14 days. The analyses revealed 470 regulated phosphopeptides (304 identified proteins) after induction of osteogenic differentiation with BMP-2 and 582 regulated phosphopeptides (376 identified proteins) after osteogenic differentiation with ODM. While the ratio of significantly increased to decreased phosphorylation was 40%–60% after induction of differentiation with ODM, this ratio was 45%–55% after induction of differentiation with BMP-2. The lists of proteins identified were further analyzed using the bioinformatics tool GENE ONTOLOGY (Tables 1 and 2) and Reactome (Tables S1 and S2). These bioinformatic analyses identified overrepresented processes that are generally related to cell organization and signal transduction. Based on the Reactome analyses, approximately 26% of all proteins that have undergone significantly regulated phosphorylation 14 days after induction of osteogenic differentiation with BMP-2 or dexamethasone are associated with signal transduction. It was also noticeable that Rho-GTPase-associated proteins were overrepresented. In addition, biological processes related to the cytoskeleton, cell cycle, and mRNA processing were identified. Proteins

TABLE 1 Gene ontology (GO) biological process (count 10 or higher) in osteogenic differentiation medium (ODM).

Term	Count
GO:0,007165~signal transduction	36
GO:0,006468~protein phosphorylation	27
GO:00,50790~regulation of catalytic activity	22
GO:00,15031~protein transport	22
GO:00,51301~cell division	21
GO:00,35556~intracellular signal transduction	21
GO:0,006915~apoptotic process	19
GO:00,43066~negative regulation of apoptotic process	18
GO:0,008380~RNA splicing	17
GO:0,006397~mRNA processing	16
GO:0,007049~cell cycle	16
GO:00,16477~cell migration	14
GO:0,006886~intracellular protein transport	14
GO:00,30036~actin cytoskeleton organization	13
GO:00,46777~protein autophosphorylation	13
GO:0,007010~cytoskeleton organization	12
GO:0000398~mRNA splicing, via spliceosome	12
GO:00,42981~regulation of apoptotic process	12
GO:00,43065~positive regulation of apoptotic process	12
GO:0000226~microtubule cytoskeleton organization	11
GO:00,90090~negative regulation of canonical Wnt signaling pathway	11
GO:00,18105~peptidyl-serine phosphorylation	11
GO:00,43123~positive regulation of I-kappaB kinase/NF-kappaB signaling	11
GO:00,43547~positive regulation of GTPase activity	10
GO:0,007507~heart development	10
GO:0,001525~angiogenesis	10

associated with apoptosis could also be identified, but with a lower priority.

Apoptosis and oxidative stress

To demonstrate the induction of cellular stress in DFCs during osteogenic differentiation, we measured cell death and oxidative stress (ROS) in DFCs after induction of osteogenic differentiation. We demonstrated the induction of cell death (Figure 1A, B) and oxidative stress (Figure 1C, D) in DFCs after induction of osteogenic differentiation with BMP-2 and ODM.

In addition, the expression of oxidative stress defense proteins was studied to investigate the importance of oxidative stress during differentiation. Expression of the oxidative stress defense protein, catalase, was increased by induction of osteogenic differentiation with both differentiation media,

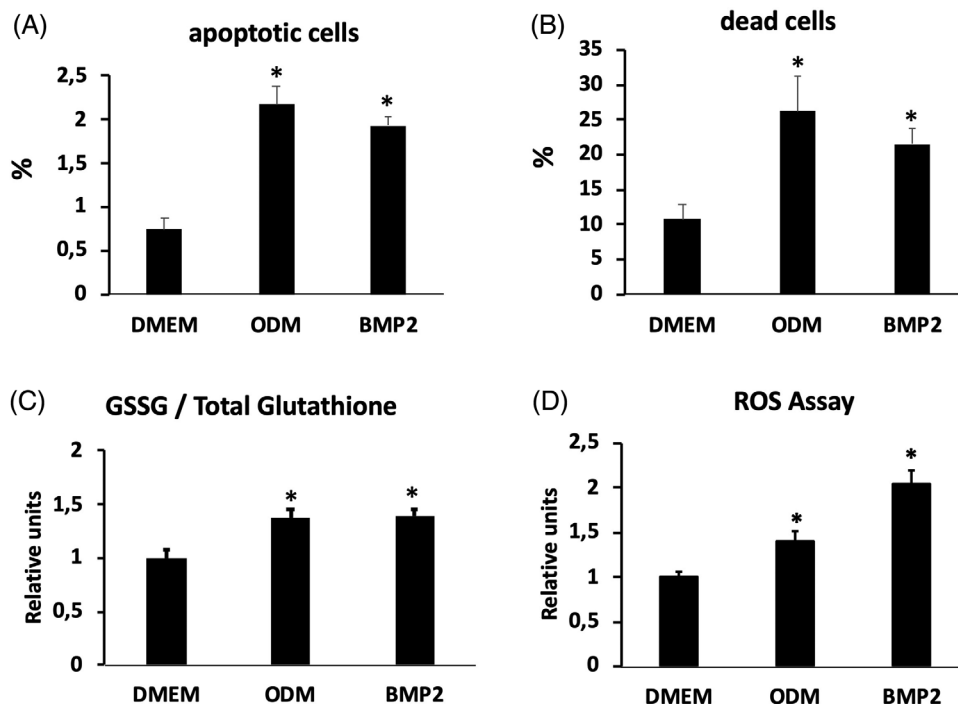


FIGURE 1 Percentage of apoptotic cells (A) and dead cells (B) measured using the cell event Caspase-3/7 green flow cytometry assay after induction of osteogenic differentiation with bone morphogenetic protein 2 (BMP-2) or dexamethasone (osteogenic differentiation medium [ODM]). Evaluation of oxidative stress was performed using the GSH/GSSG-Glo assay kit (C) and evaluation of reactive oxidative species (ROS) was performed using flow cytometry (D) after induction of osteogenic differentiation with BMP-2 or dexamethasone (ODM). DMEM, Dulbecco’s minimal essential medium (control; no stimulation of osteogenic differentiation); GSSG, glutathione disulfide; ROS, reactive oxygen species. All bars are mean ± SD ($n = 3$). * $p < 0.05$ (compared with control group; Student’s t -test).

TABLE 2 Gene ontology (GO) biological process (count 10 or higher) in bone morphogenetic protein 2 (BMP-2) differentiation medium.

Term	Count
GO:0,007165~signal transduction	30
GO:00,35556~intracellular signal transduction	19
GO:0,006468~protein phosphorylation	18
GO:00,50790~regulation of catalytic activity	17
GO:00,51301~cell division	16
GO:00,15031~protein transport	15
GO:0,006397~mRNA processing	14
GO:0,008380~RNA splicing	13
GO:0,007049~cell cycle	13
GO:0,006886~intracellular protein transport	12
GO:00,43065~positive regulation of apoptotic process	12
GO:00,51056~regulation of small GTPase mediated signal transduction	11
GO:0,007010~cytoskeleton organization	10
GO:00,43547~positive regulation of GTPase activity	10
GO:00,98609~cell-cell adhesion	10
GO:0000398~mRNA splicing, via spliceosome	10

but expression was significantly stronger after induction by BMP-2 (Figure 2A). Inhibition of catalase with 3-AT (10 mM) reduced the biomineralization of DFCs in the differentiation medium containing dexamethasone (Figure 2B) but not in the that containing BMP-2 (data not shown).

Another interesting observation was that the inhibition of AKT, whose importance during differentiation has already been investigated [15], could also be detected in the phosphoproteome after differentiation was induced by incubation in BMP-2 medium. Furthermore, we were able to show that inhibition of AKT prevents the formation of ROS in DFCs (Figure 2C), partially supporting the regulation of ROS during osteogenic differentiation.

DISCUSSION

In this study we examined the phosphoproteome of DFCs on day 14 after induction of osteogenic differentiation with either BMP-2 or dexamethasone (ODM). Identified regulated proteins at this phase of osteogenic differentiation revealed similar biological processes, such as signal transduction, mRNA processing, the cell cycle, and cytoskeleton organization. Searching for signaling pathways and biological processes using Reactome showed that regulated proteins

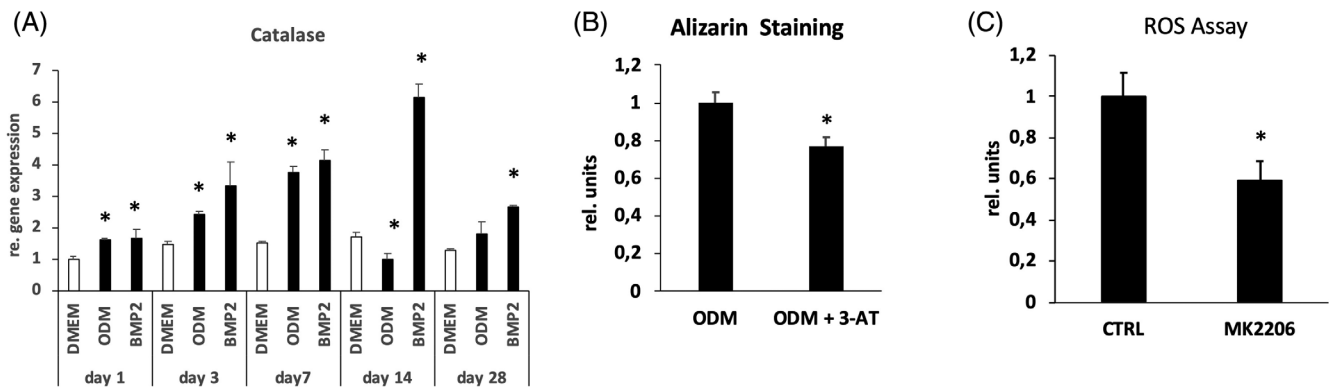


FIGURE 2 (A) Measurement of relative gene expression of the catalase gene (*CAT*) in dental follicle cells (DFCs), 1, 3, 7, 14, and 28 days after induction of osteogenic differentiation with dexamethasone (osteogenic differentiation medium [ODM]) or bone morphogenetic protein 2 (BMP-2). DMEM, Dulbecco's modified essential medium (control; no induction of osteogenic differentiation). (B) Alizarin red staining (indicating biomineralization) 4 weeks after induction of osteogenic differentiation in DFCs with dexamethasone (ODM), with and without 3-amino-1,2,4-triazole (3-AT) (10 mM), an inhibitor of catalase. (C) Flow cytometric evaluation of reactive oxidative species (ROS) in DFCs, with and without inhibitor of AKT (MK2206; 200 nM). All bars are mean \pm SD ($n = 3$); * $p < 0.05$, Student's *t*-test, (compared with the control group).

during osteogenic differentiation are associated with the group of Rho-GTPase protein kinases. These protein kinases are very often associated with the differentiation of stem cells. Santos et al. showed, for example, that WNT5A, which is also associated with osteogenic differentiation of DFCs [15, 21, 22], induces osteogenic differentiation of human adipose stem cells via the Rho-associated kinase Rock, which alters the actin cytoskeleton [23]. Crucial effects of Rock in cytoskeletal reorganization and osteogenic differentiation were also shown in periodontal ligament stem cells [24]. In addition, simvastatin acts similarly via the RhoA signaling pathway as an inducer of osteogenic differentiation with increased organization of actin filaments and cell rigidity [16]. However, the Rho/ROCK pathway appears to be a general mediator for cell differentiation as it is also involved in tendon differentiation in mesenchymal stem cells [25].

While cytoskeletal changes are more than likely based on obtained proteomic data and our previous observations [26], in this study we focused on apoptosis and oxidative stress in DFCs during differentiation. Apoptosis and ROS can be induced or regulated via cytoskeletal changes and/or proteins from the group of Rho-GTPases [27, 28] and were significantly elevated after the induction of osteogenic differentiation of DFCs. Identified and regulated proteins in this study showed, it was apparent that proteins involved in biological signaling pathways such as 'apoptosis', 'programmed cell death', or 'intracellular signaling by second messengers' were overrepresented. An identified protein that was regulated after differentiation with BMP-2 and is also involved in the biological pathway of apoptosis, is AKT, which is regulated during osteogenic differentiation. In a previous study, we showed that inhibition of AKT enhances differentiation with BMP-2 [15]. We have now shown that inhibition of AKT inhibits the forma-

tion of ROS in DFCs and that inhibition of the oxidative stress defense protein, catalase, prevents the osteogenic differentiation of DFCs. These data support our initial assumption that regulation of oxidative stress or ROS is involved in the process of osteogenic differentiation. It is also believed that regulation of ROS supports differentiation of mesenchymal stem cells into osteoblasts, while increased levels of ROS support adipogenic differentiation [29]. Further studies have shown that inhibition of ROS by *N*-acetylcysteine and hypoxia induced by succinate support osteogenic differentiation of osteogenic progenitor cells [30, 31].

In conclusion, our study provides new information on the mechanisms of the later phase of osteogenic differentiation of DFCs. In connection with the results of our previous study [17], during this differentiation phase metabolic processes are induced in DFCs that increase oxidative stress that need to be regulated. It remains unclear to what extent the signaling pathways associated with the Rho-GTPases are involved in the differentiation and regulation of oxidative stress. Proteins from these signaling pathways were grossly overrepresented, but only more sophisticated future studies will provide new insights in this area.

AUTHOR CONTRIBUTIONS

Conceptualization: Christian Morszeck; **Methodology:** Oliver Pieles, Hans-Christian Beck; **Validation:** Oliver Pieles, Hans-Christian Beck; **Formal Analysis:** Christian Morszeck, Oliver Pieles, Hans-Christian Beck; **Investigation:** Oliver Pieles, Hans-Christian Beck; **Data Curation:** Hans-Christian Beck; **Funding acquisition:** Christian Morszeck; **Writing-Original Draft Preparation:** Christian Morszeck, Hans-Christian Beck; **Writing-Review & Editing:** Christian Morszeck, Oliver Pieles, Hans-Christian Beck.

ACKNOWLEDGMENTS

This work was supported by a grant of the Deutsche Forschungsgemeinschaft (DFG project MO1875/10-3; project number 319,390,412).

Open access funding enabled and organized by Projekt DEAL.

CONFLICT OF INTEREST STATEMENT

The authors declare no conflict of interest.


DATA AVAILABILITY STATEMENT

All data that support the findings of this study are available upon request from the corresponding author. All authors take responsibility for the integrity of the data and the accuracy of the data analysis.

ORCID

Christian Morsczeck  <https://orcid.org/0000-0002-3580-5883>

Oliver Pieves  <https://orcid.org/0000-0002-7901-1057>

Hans-Christian Beck  <https://orcid.org/0000-0002-7763-3637>

REFERENCES

1. Ten Cate AR. The development of the periodontium—a largely ectomesenchymally derived unit. *Periodontol* 2000. 1997;13:9-19.
2. Diekwisch TG. The developmental biology of cementum. *Int J Dev Biol*. 2001;45:695-706.
3. Morsczeck C, Gotz W, Schierholz J, Zeilhofer F, Kuhn U, Mohl C, et al. Isolation of precursor cells (PCs) from human dental follicle of wisdom teeth. *Matrix Biol*. 2005;24:155-65.
4. Luan X, Ito Y, Dangaria S, Diekwisch TG. Dental follicle progenitor cell heterogeneity in the developing mouse periodontium. *Stem Cells Dev*. 2006;15:595-608.
5. Kemoun P, Narayanan AS, Brunel G, Salles JP, Laurencin-Dalieux S, Rue J, et al. Human dental follicle cells acquire cementoblast features under stimulation by BMP-2/-7 and enamel matrix derivatives (EMD) in vitro. *Cell Tissue Res*. 2007;329:283-94.
6. Saugspier M, Felthaus O, Viale-Bouroncle S, Driemel O, Reichert TE, Schmalz G, et al. The differentiation and gene expression profile of human dental follicle cells. *Stem Cells Dev*. 2010;19:707-17.
7. Park GT, Morasso MI. Bone morphogenetic protein-2 (BMP-2) transactivates Dlx3 through Smad1 and Smad4: alternative mode for Dlx3 induction in mouse keratinocytes. *Nucleic Acids Res*. 2002;30:515-22.
8. Hassan MQ, Javed A, Morasso MI, Karlin J, Montecino M, van Wijnen AJ, et al. Dlx3 transcriptional regulation of osteoblast differentiation: temporal recruitment of Msx2, Dlx3, and Dlx5 homeodomain proteins to chromatin of the osteocalcin gene. *Mol Cell Biol*. 2004;24:9248-61.
9. Viale-Bouroncle S, Felthaus O, Schmalz G, Brockhoff G, Reichert TE, Morsczeck C. The transcription factor DLX3 regulates the osteogenic differentiation of human dental follicle precursor cells. *Stem Cells Dev*. 2012;21:1936-47.
10. Hassan MQ, Tare RS, Lee SH, Mandeville M, Morasso MI, Javed A, et al. BMP2 commitment to the osteogenic lineage involves activation of Runx2 by DLX3 and a homeodomain transcriptional network. *J Biol Chem*. 2006;281:40515-26.
11. Morsczeck C. Mechanisms during osteogenic differentiation in human dental follicle cells. *Int J Mol Sci*. 2022;23:5945. <https://doi.org/10.3390/ijms23115945>
12. Morsczeck C, Reck A, Beck HC. The hedgehog-signaling pathway is repressed during the osteogenic differentiation of dental follicle cells. *Mol Cell Biochem*. 2017;428:79-86.
13. Klingelhöffer C, Reck A, Ettl T, Morsczeck C. The parathyroid hormone-related protein is secreted during the osteogenic differentiation of human dental follicle cells and inhibits the alkaline phosphatase activity and the expression of DLX3. *Tissue Cell*. 2016;48:334-9.
14. Pieves O, Reck A, Morsczeck C. High endogenous expression of parathyroid hormone-related protein (PTHrP) supports osteogenic differentiation in human dental follicle cells. *Histochem Cell Biol*. 2020;154:397-403.
15. Pieves O, Reichert TE, Morsczeck C. Classical isoforms of protein kinase C (PKC) and Akt regulate the osteogenic differentiation of human dental follicle cells via both beta-catenin and NF-kappa B. *Stem Cell Res Ther*. 2021;12:242. <https://doi.org/10.1186/s13287-021-02313-w>
16. Tai IC, Wang YH, Chen CH, Chuang SC, Chang JK, Ho ML. Simvastatin enhances Rho/actin/cell rigidity pathway contributing to mesenchymal stem cells' osteogenic differentiation. *Int J Nanomed*. 2015;10:5881-94.
17. Pieves O, Hoering M, Adel S, Reichert TE, Liebisch G, Morsczeck C. Energy metabolism and lipidome are highly regulated during osteogenic differentiation of dental follicle cells. *Stem Cells Int*. 2022;2022:3674931. <https://doi.org/10.1155/2022/3674931>
18. Winer J, Jung CK, Shackel I, Williams PM. Development and validation of real-time quantitative reverse transcriptase-polymerase chain reaction for monitoring gene expression in cardiac myocytes in vitro. *Anal Biochem*. 1999;270:41-9.
19. Dennis G, Sherman BT, Hosack DA, Yang J, Gao W, Lane HC, et al. DAVID: database for annotation, visualization, and integrated discovery. *Genome Biol*. 2003;4:P3.
20. Haw R, Hermjakob H, D'Eustachio P, Stein L. Reactome pathway analysis to enrich biological discovery in proteomics data sets. *Proteomics*. 2011;11:3598-613.
21. Xiang L, Chen M, He L, Cai B, Du Y, Zhang X, et al. Wnt5a regulates dental follicle stem/progenitor cells of the periodontium. *Stem Cell Res Ther*. 2014;5:135. <https://doi.org/10.1186/scrt525>
22. Morsczeck C, Reck A, Reichert TE. WNT5A supports viability of senescent human dental follicle cells. *Mol Cell Biochem*. 2019;455:21-8.
23. Santos A, Bakker AD, de Blicke-Hogervorst JM, Klein-Nulend J. WNT5A induces osteogenic differentiation of human adipose stem cells via rho-associated kinase ROCK. *Cytotherapy*. 2010;12:924-32.
24. Yamamoto T, Ugawa Y, Yamashiro K, Shimoe M, Tomikawa K, Hongo S, et al. Osteogenic differentiation regulated by Rho-kinase in periodontal ligament cells. *Differentiation*. 2014;88:33-41.
25. Maharam E, Yaport M, Villanueva NL, Akinyibi T, Laudier D, He ZY, et al. Rho/Rock signal transduction pathway is required for MSC tenogenic differentiation. *Bone Res*. 2015;3:15015. <https://doi.org/10.1038/boneres.2015.15>
26. Viale-Bouroncle S, Völlner F, Möhl C, Küpper K, Brockhoff G, Reichert TE, et al. Soft matrix supports osteogenic differentiation

- of human dental follicle cells. *Biochem Biophys Res Commun.* 2011;410:587-92.
27. Coleman ML, Olson MF. Rho GTPase signalling pathways in the morphological changes associated with apoptosis. *Cell Death Differ.* 2002;9:493-504.
28. MacKay CE, Shaifta Y, Snetkov VV, Francois AA, Ward JPT, Knock GA. ROS-dependent activation of RhoA/Rho-kinase in pulmonary artery: role of Src-family kinases and ARHGEF1. *Free Radic Biol Med.* 2017;110:316-31.
29. Atashi F, Modarressi A, Pepper MS. The role of reactive oxygen species in mesenchymal stem cell adipogenic and osteogenic differentiation: a review. *Stem Cells Dev.* 2015;24:1150-63.
30. Mao H, Yang A, Zhao Y, Lei L, Li H. Succinate supplement elicited "Pseudohypoxia" condition to promote proliferation, migration, and osteogenesis of periodontal ligament cells. *Stem Cells Int.* 2020;2020:2016809. <https://doi.org/10.1155/2020/2016809>
31. Wang YN, Jia TT, Feng Y, Liu SY, Zhang WJ, Zhang DJ, et al. Hyperlipidemia impairs osseointegration via the ROS/Wnt/beta-catenin pathway. *J Dent Res.* 2021;100:658-65.

SUPPORTING INFORMATION

Additional supporting information can be found online in the Supporting Information section at the end of this article.

How to cite this article: Morszeck C, Pielek O, Beck H-C. Analysis of the phosphoproteome in human dental follicle cells during osteogenic differentiation. *Eur J Oral Sci.* 2023;e12952. <https://doi.org/10.1111/eos.12952>